Crystal Engineering Using the Unconventional Hydrogen Bond. Synthesis, Structure, and Theoretical Investigation of Cyclotrigallazane

John P. Campbell,[†] Jen-Wei Hwang,[†] Victor G. Young, Jr.,[†] Robert B. Von Dreele,[‡] Christopher J. Cramer,*[,†] and Wayne L. Gladfelter*[,†]

Contribution from the Department of Chemistry, University of Minnesota, Minneapolis, Minnesota 55455, and LANSCE, MS-H805 Los Alamos National Laboratory, Los Alamos, New Mexico 87545

Received May 7, 1997

Abstract: Cyclotrigallazane, $[H_2GaNH_2]_3$, was prepared by condensing liquid ammonia onto solid trimethylamine gallane, $GaH_3(NMe_3)$, at −78 °C and allowing the mixture to warm to room temperature and was characterized by IR, mass spectroscopy, elemental analysis, single-crystal X-ray, and neutron powder diffraction. Single-crystal X-ray diffraction at $T = -167$ °C established that the $(GaN)_3$ ring was in the chair conformation. Neutron powder diffraction data collected at 25 °C on the fully deuterated analogue were analyzed with Rietveld refinement to give an average bond distance for Ga−D of 1.56(3) Å and a N−D of 1.04(5) Å. The intermolecular interactions were dominated by four Ga−H···H−N unconventional hydrogen bonds per molecule that form a chain parallel to the crystallographic *a* axis. The crystallographically equivalent D···D bond lengths are 1.97 Å. Calculations revealed that in the gas phase, twist-boat conformations are preferred over chairs for cyclotrigallazane and the related boron and aluminum compounds by 0.9 to 2.6 kcal/mol at correlated levels of electronic structure theory. For cyclotriborazane and cyclotrigallazane, calculations suggest that each H···H hydrogen bond contributes about 3 kcal/mol to the binding energy (relative to the chair monomer); this value is very slightly higher for cyclotrialumazane.

Introduction

Hydrogen bonds are used extensively as a tool to design the structure of molecular crystals, in part because of their strength relative to other intermolecular, noncovalent interactions.[1−5] In addition a rough ranking exists of the energies of H-bonds from the strongest bond in FHF^- at 30 kcal/mol[6] to much weaker C−H···X interactions.[7−10] Typical values of X−H···Y bonds where X and Y are oxygen and/or nitrogen range from 3 to 10 kcal/mol.[6]

The so-called unconventional hydrogen bond, a bond between hydrogens of opposite polarity, has recently attracted attention.[11] Crabtree and co-workers have enumerated several examples of unconventional hydrogen bonds involving transition metal hydrides[12,13] and have summarized some of the literature associated with B−H···H−N interactions.[14] In the typical geometry, shown in Scheme 1, the BH and HN vectors are usually not collinear, and the close, noncovalently bonded H···H distances typically range from 2.0 to 2.4 Å.

The strength of these weak bonds is expected to increase with increasing polarity differences and theoretical predictions have estimated a value of 5−6 kcal/mol in various model systems—similar to classical H-bonds.[14,15] Examples with main group metal hydrides extend beyond the intermolecular interactions to include intramolecular H···H bonds, resulting, for example, in the observed eclipsed geometry in the donor−acceptor complex between tetramethylpiperidine and alane (AlH_3).[16]

In this paper, we describe the synthesis and structure of $[H_2GaNH_2]_3$, which exhibits close intermolecular distances characteristic of unconventional H···H bonds. Theoretical calculations are used to evaluate the strength of these interactions for the corresponding boron, aluminum, and gallium compounds and have also suggested that the gas-phase structures of the monomers prefer to exist in twist-boat conformations. The strength of the intermolecular interaction suggests that unconventional hydrogen bonds may be important contributors to the

[†] University of Minnesota.
[‡] Los Alamos National Laboratory.

(1) Desiraju, G. R. *Crystal Engineering*; Elsevier: New York, 1989; p 312.
(2) Etter, M. C. *Acc. Chem. Res.* **1990**, *23*, 120.
(3) Chang, Y.-L.; West, M.-A.; Fowler, F. W.; Lauher, J. W. *J. Am. Chem. Soc.* **1993**, *115*, 5991.
(4) Lehn, J.-M. *Supramolecular Chemistry*; VCH: New York, 1995; p 271.
(5) Whitesides, G. M.; Mathias, J. P.; Seto, C. T. *Science* **1991**, *254*, 1312.
(6) Wells, A. F. *Structural Inorganic Chemistry*, 5th ed.; Oxford University Press: Oxford, 1984; p 1382.
(7) Sarma, J. A. R. P.; Desiraju, G. R. *Acc. Chem. Res.* **1986**, *19*, 222.
(8) Padilla-Martinez, I.; Rosalez-Hoz, M.; Tlahuext, H.; Camacho-Camacho, C.; Ariza-Castolo, A.; Contreras, R. *Chem. Ber.* **1996**, *129*, 441.
(9) Desiraju, G. R. *Acc. Chem. Res.* **1996**, *29*, 441.
(10) Steiner, T. *J. Chem. Soc., Chem. Commun.* **1997**, 727.
(11) Crabtree, R.; Siegbahn, P.; Eisenstein, O.; Rheingold, A.; Koetzle, T. *Acc. Chem. Res.* **1996**, *29*, 348.
(12) Wessel, J.; Lee, J. C.; Peris, E.; Yap, G. P. A.; Fortin, J. B.; Ricci, J. S.; Sini, G.; Albinati, A.; Koetzle, T. F.; Eisenstein, O.; Rheingold, A.; Crabtree, R. H. *Angew. Chem., Int. Ed. Engl.* **1995**, *34*, 2507.
(13) Patel, B. P.; Wessel, J.; Yao, W.; Lee, J. C., Jr.; Peris, E.; Koetzle, T. F.; Yap, G. P. A.; Fortin, J. B.; Ricci, J. S.; Sini, G.; Albinati, A.; Eisenstein, O.; Rheingold, A. L.; Crabtree, R. H. *New J. Chem.* **1997**, *21*, 413.
(14) Richardson, T. B.; de Gala, S.; Crabtree, R. H.; Siegbahn, P. E. M. *J. Am. Chem. Soc.* **1995**, *117*, 12875.
(15) Cramer, C. J.; Gladfelter, W. L. *Inorg. Chem.* **1997**, *36*, 5358.

S0002-7863(97)01478-9 CCC: $15.00
Published on Web 01/08/1998

Scheme 1

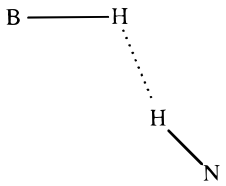

structure of the molecular solids in much the same fashion as found for classic H-bonding. The structure of $[H_2GaNH_2]_3$, described in this paper, provides strong evidence for this suggestion. A preliminary report on the synthesis of cyclotrigallazane and a separate study of its conversion to nanocrystalline GaN have appeared.[17,18]

Experimental/Computational Methods

General. Air and moisture were excluded from all reactions through the use of standard Schlenk techniques or a nitrogen filled glovebox (Vacuum Atmospheres Company, Dri-Train Model 40-1). All solvents were dried and freshly distilled before use. $(GaH_3)NMe_3$ and $(GaD_3)NMe_3$ were prepared following the literature method.[19,20] Ammonia (Matheson) and ammonia-d_3 (Cambridge Isotope Laboratories) were used as received.

Infrared spectra were recorded on a Mattson Cygnus 25 FTIR spectrometer equipped with a HgCdTe detector. Low resolution mass spectra were recorded with either an AEI MS-30 or a VG-7070E/HF mass spectrometer. Samples were placed into capillary tubes in the drybox with the protection of grease on the top and were sealed off shortly after being removed from the box. Minimum exposure of the samples to air was achieved by quickly breaking and loading the capillary tube into the solid probe. X-ray powder diffraction studies were conducted on a Siemens D500 diffractometer with monochromatic (graphite) Cu Ka radiation. Elemental analysis of cyclotrigallazane was done by Analytische Laboratorien, Engelskirchen, Germany.

Synthesis of $[H_2GaNH_2]_3$. Trimethylamine gallane (0.525 g, 4 mmol) was charged to a 100 mL Schlenk flask, the flask was cooled to −196 °C, under vacuum, and approximately 1 mL (45 mmol) of liquid ammonia was condensed on top of the gallane. The flask was then filled with N_2, and the mixture was slowly warmed to −78 °C, and then ultimately to room temperature. Excess ammonia was purged with a stream of N_2. A white solid was isolated: yield 0.25 g, 72% (isolated). A melting point was not observed up to 150 °C. IR (Nujol mull): 3299, 3246, 1889, 1865, 1833, 1525, 1512, 977, 958, 740, 711, 681, and 651 cm^{-1}. MS (EI, 20 eV) *m*/*e* (relative abundance, ion): 262 (24%, P-1), 173 (100%, P-90). Anal. Calcd: Ga, 79.70; N, 15.71; H, 15.96; H, 4.59; C, 0.00. Found: Ga, 79.70; N, 15.71; H, 4.46; C, 0.08. The same product can also be obtained by direct reaction of gaseous ammonia over solid $(GaH_3)NMe_3$ at room temperature.

Synthesis of $[D_2GaND_2]_3$. Two equivalents of ND_3 were condensed on to $(GaD_3)NMe_3$ (3.07 g, 22.8 mmol) cooled to liquid N_2 temperature. The mixture was then slowly warmed to −78 °C and eventually room temperature over 2 h. The reaction mixture bubbled very slowly at ca. −25 °C and turned cloudy at ca. −10 °C. A white solid was isolated (1.82 g, 87% yield). IR (*n*-undecane mull): $\nu_{N-D(obsd)}$ 2462, 2386 cm^{-1}; $\nu_{Ga-D(obsd)}$ 1360, 1343, 1323 cm^{-1}. MS (EI, 20 eV) *m*/*e* (relative abundance, ion): 273 (43%, P-2), 182 (100%, P-91).

X-ray Crystallographic Studies. Crystals of $[H_2GaNH_2]_3$ were obtained by sublimation of the material at 80−87 °C at 0.05 Torr. The crystals were small—typically less than 0.26 mm in the largest dimension. In a glovebox they were transferred to a glass plate and covered with a heavy hydrocarbon oil to minimize their exposure to the atmosphere. A suitable crystal was selected and mounted on the tip of a glass fiber with STP oil. It was transferred to the goniometer of a Siemens SMART CCD System and cooled to −167 °C with a Siemens LT-2 low-temperature device. Crystal quality and centering was confirmed by taking a 60-s rotation frame. A search was performed by taking a series of frames in three orthogonally related regions of reciprocal space. Each region investigated comprised thirty 30-s frames, 0.3° apart in ω. These were harvested to yield a total of about 35 reflections with intensities greater than 10σ. An initial unit cell was obtained, and checked for centering and higher symmetry. None was found. The initial cell constants were refined, and an initial orientation matrix was determined. Data were collected by examining a randomly oriented region of reciprocal space in three segments; the frames collected in a given segment were 0.3° apart in ω. The highest resolution data collected was 0.87 Å. Two 30-s frames were collected, and the data were summed, doubling the dynamic range of the detector. The default gain on the detector signal was 4×, which was automatically dropped to 1× when the detector range was exceeded. Final cell constants were determined during integration of the data using 1722 intense, well-centered reflections.

A solution was attempted via direct methods in the space group $P2_1$ with use of the SHELXTL 5.0 series of programs.[21] A direct methods solution was obtained, but refinement would not proceed without the structure "breaking up". A solution was obtained in $P2_1/m$, and isotropic refinement proceeded successfully. All non-hydrogen atoms were located immediately in the difference map. Refinement and subsequent difference maps revealed the location of the hydrogen atoms attached to the Ga atoms. Hydrogens attached to the nitrogens were placed in calculated (N−H = 0.92 Å) positions and allowed to refine with *B* values 20% greater than those for the atoms to which they were attached. Hydrogens attached to the gallium atoms were placed in calculated (Ga−H = 1.56 Å) positions and allowed to refine isotropically. Full anisotropic refinement on F^2 of the non-hydrogen atoms then proceeded. Refinement without the twin law yielded an R_1 value of 11%. In SHELXTL, the effects of twinning are incorporated into the structure factor expression by using the method of Pratt.[22,23] With the twinning accounted for, the refinement converged at $R_1 = 0.035$ (4σ, based on F^2). The batch scale factor (BASF) indicating the contribution of the twin components to each structure factor was 0.43, indicating a 0.57/0.43 twin. The twin law used was

$$\begin{bmatrix} \bar{1} & 0 & 0 \\ 0 & 0 & \bar{1} \\ 1 & 0 & 1 \end{bmatrix}$$

At this point, a semiempirical ψ-scan type absorption correction was applied. Due to the twinning, the 2/m Laue symmetry was broken. The absorption correction was applied on the basis of 1200 reflections, assuming a Laue symmetry of $\bar{1}$. Further refinement yielded a final $R_1 = 0.0245$ (4σ, based on F^2). The final difference map was essentially flat, with maximum and minimum peaks corresponding to 1.288 and −0.933 $e^-/Å^3$. Scattering factors and anomalous scattering terms were taken from the usual sources,[24] and the effects of anomalous dispersion were included for the non-hydrogen atoms.

Over the course of this project a complete set of data was collected for seven crystals—all showed the same twinning. The crystal used for the results reported above had the largest difference between the two twin fragments. Details of the data collection are given in Table 1, and positional parameters and isotropic thermal factors are given in the Supporting Information. A thermal ellipsoid diagram is shown in Figure 1.

X-ray Powder Diffraction of Cyclotrigallazane. In a glovebox, powders of bulk cyclotrigallazane were placed onto an X-ray sample plate. Scotch tape was placed over the sample to protect it from air. The sample was then placed into a plastic bag that was then ziplocked.

(16) Atwood, J. L.; Koutsantonis, G. A.; Lee, F.-C.; Raston, C. L. *J. Chem. Soc., Chem. Commun.* **1994**, 91.
(17) Hwang, J.-W.; Hanson, S. A.; Britton, D.; Evans, J. F.; Jensen, K. F.; Gladfelter, W. L. *Chem. Mater.* **1990**, *2*, 342.
(18) Hwang, J.-W.; Campbell, J. P.; Kozubowski, J.; Hanson, S. A.; Evans, J. F.; Gladfelter, W. L. *Chem. Mater.* **1995**, *7*, 517.
(19) Shriver, D. F.; Parry, R. W. *Inorg. Chem.* **1963**, *2*, 1039.
(20) Shriver, D. F.; Shirk, A. E. *Inorg. Synth.* **1977**, *17*, 42.
(21) Sheldrick, G. *SHELXTL Plus, 5.0*; Siemens Analytical X.-Ray Instrumentation, Inc.: Madison, WI, 1994.
(22) Pratt, C.; Coyle, B.; Ibers, J. *J. Chem. Soc.* **1971**, 2146.
(23) Jameson, G. *Acta Crystallogr.* **1982**, *A38*, 817.
(24) *International Tables for Crystallography*; Wilson, A. J. C., Ed.; Kluwer Academic Publishers: Dordrecht, The Netherlands, 1995; Tables 4.

Table 1. Crystal Data, Collection, and Solution and Refinement Parameters for $[H_2GaNH_2]_3$[a]

empirical formula	$Ga_3N_3H_{12}$
crystal habit, color	arrowhead, colorless
crystal size	0.26 × 0.16 × 0.12 mm
crystal system	monoclinic
space group	$P2_1/m$
unit cell dimens	
a	5.7615(5) Å [5.7893(4) Å]
b	8.5079(7) Å [8.5635(4) Å]
c	8.0848(6) Å [8.1617(6) Å]
β	110.843(2)° [111.038(6)°]
volume	370.37(5) Å^3 [377.66(3) Å^3]
Z	2
formula wt	263.29
density (calcd)	2.361 mg/m^3
abs coeff	10.728 mm^{-1}
$F_{(000)}$	252
diffractometer	Siemens SMART Platform CCD
wavelength	0.710 73 Å
temperature	106(2) K
θ range for data collection	2.39 to 24.13°
index ranges	$-6 < h < 6, -9 < k < 9, -9 < l < 5$
no. of reflcns collected	1853
no. of independent reflcns	639 ($R_{int} = 0.0379$)
system used	SHELXTL-V5.0
solution	direct methods
refinement method	full-matrix least-squares on F^2
weighting scheme	$w = [s^2(F_o^2) + (0.0412P)^2 + (0.5560P)]^{-1}$, where $P = (F_o^2 + 2F_c^2)/3$
abs corr	semiempirical
max and min transmission	0.955, 0.450
data/restraints/parameters	639/0/38
final *R* indices [$I > 2\sigma(I)$]	$R_1 = 0.0240$, $wR_2 = 0.0621$
R indices (all data)	$R_1 = 0.0242$, $wR_2 = 0.0623$
goodness-of-fit on F^2	1.074
largest diff peak and hole	1.288 and −0.933 e$^-$/Å^3

[a] Unit cell dimensions in brackets refer to the neutron diffraction data for $[D_2GaND_2]_3$ collected at 25 °C. A complete list of the neutron powder diffraction refinement parameters appears in the Supporting Information.

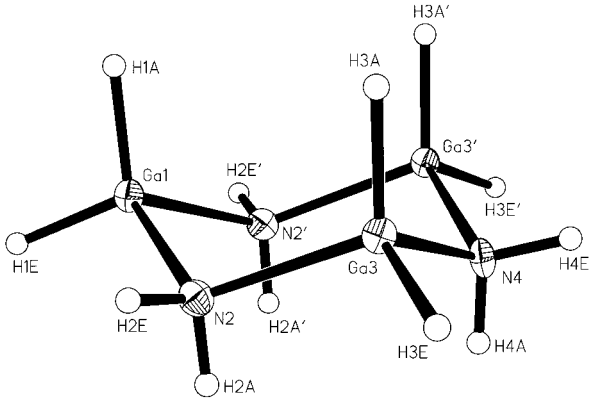

Figure 1. Structure of cyclotrigallazane as determined by the single-crystal X-ray diffraction study. The thermal ellipsoids for the Ga and N atoms are shown at the 50% level.

The sample was removed immediately prior to data collection. Despite these efforts, the sample was slowly oxidized to an amorphous material within an hour.

Neutron Powder Diffraction of $[D_2GaND_2]_3$. In a nitrogen-filled glovebox, a thin-walled vanadium container (7 mm × 50 mm) was packed with approximately 1 g of $[D_2GaND_2]_3$. Time-of-flight (TOF) neutron powder diffraction data were collected on the High-Intensity Powder Diffractometer (HIPD) at the Manuel Lujan Neutron Scattering Center (LANSCE) at Los Alamos National Laboratory. Tables 1 and 2 include the refined crystal parameters and bond lengths and angles, respectively. Details of the data collection are given in the Supporting Information. Refinement of the neutron data was performed with the program GSAS.[25] The unit cell, unit cell contents, space group, and atom positions used for the trial structure were derived from the previously determined single-crystal X-ray structure. Due to the poor quality of the data, only data between 0.8 and 3.0 Å resolution were included in the refinement. Data below 0.8 Å were too near background to yield a refinable profile, and data above 3.0 Å were too noisy to give well-determined reflections. Soft restraints were applied in the initial stages of refinement to keep the refinement from diverging. These were loosened as the refinement progressed. The hydrogen atoms were placed in estimated positions and allowed to refine to their most stable positions. In the case of D4B, which had a *B* value of 0.095, the atom was removed and a Fourier difference map was used to confirm the position.

Table 2. Experimental and Calculated Bond Lengths (Å) and Angles (deg) for $[H_2GaNH_2]_3$ (XRD) and $[D_2GaND_2]_3$ (ND)

atoms	$[H_2GaNH_2]_3$	$[D_2GaND_2]_3$	calcd[a]
Ga1−N2′	1.987(4)	1.975(7)	2.010
Ga1−N2	1.987(4)	1.975(7)	2.010
Ga1−H1A	1.40(6)	1.56(1)	1.564
Ga1−H1E	1.40(6)	1.54(1)	1.576
N2−Ga3	1.972(4)	1.968(7)	2.010
N2−H2A	0.91(5)	1.089(9)	1.012
N2−H2E	0.91(5)	0.994(9)	1.014
Ga3−N4	1.975(3)	1.984(7)	2.010
Ga3−H3A	1.43(5)	1.590(9)	1.564
Ga3−H3E	1.43(5)	1.538(9)	1.576
N4−Ga3′	1.975(3)	1.984(7)	2.010
N4−H4A	0.91(6)	1.00(1)	1.012
N4−H4E	0.91(6)	1.057(8)	1.014
N2′−Ga1−N2	99.9(3)	93.2(7)	102.6
N2′−Ga1−H1A	111.8(1)	108.4(8)	108.4
N2−Ga1−H1A	111.8(1)	108.4(8)	108.4
N2′−Ga1−H1E	111.8(1)	112.0(7)	106.8
N2−Ga1−H1E	111.78(1)	112.0(7)	106.8
H1A−Ga1−H1E	109.5	120(1)	122.0
Ga1−N2−Ga3	116.9(2)	121.0(7)	123.7
Ga1−N2−H2A	108.1(1)	108(1)	109.0
Ga3−N2−H2A	108.1(1)	121(1)	109.0
Ga1−N2−H2E	108.1(1)	103(1)	104.9
Ga3−N2−H2E	108.1(1)	104(1)	104.9
H2A−N2−H2E	107.3	94(1)	103.7
N4−Ga3−N2	100.6(2)	95.4(7)	102.6
N4−Ga3−H3A	111.7(2)	111.6(9)	109.0
N2−Ga3−H3A	111.7(1)	107.7(7)	109.0
N4−Ga3−H3E	111.7(1)	109.3(6)	104.9
N2−Ga3−H3E	111.7(1)	114.1(8)	104.9
H3A−Ga3−H3E	109.4	116.7(9)	122.0
Ga3−N4−Ga3′	117.3(3)	119.3(9)	123.7
Ga3−N4−H4A	108.0(2)	110(1)	109.0
Ga3′−N4−H4A	108.0(2)	110(1)	109.0
Ga3−N4−H4E	108.0(2)	111(1)	104.9
Ga3′−N4−H4E	108.0(2)	111(1)	104.9
H4A−N4−H4E	107.2	91(2)	103.3

[a] RHF/ECP level.

The model profile used was that of Jorgensen and Von Dreele.[23,24] Refinement of σ_1 indicated significant Lorentzian strain, and refinement of σ_2 indicated little Scherrer broadening. The absorption correction was applied and refined to $a = 0.0598$. Preferred orientation was modeled with the March-Dollase function;[26,27] application to the [11$\bar{1}$] direction gave a preferred orientation ratio of 1.02. Isotropic refinement converged with $R_p = 0.0367$ ($wR_p = 0.0487$) with 12 soft restraints. The observed powder diffraction data, fit to the data, and difference curve are shown in Figure 2.

Calculations. Geometries for all species were fully optimized at the restricted Hartree−Fock (RHF) level of theory and electron correlation was accounted for via second-order perturbation theory

(25) Larson, A. C.; Von Dreele, R. B. *General Structure Analysis System—GSAS*, Los Alamos National Laboratory, Report LA-UR 86-748, 1994.
(26) March, A. *Z. Kristall.* **1932**, *81*, 285.
(27) Dollase, W. *J. Appl. Crystallogr.* **1986**, *19*, 267.

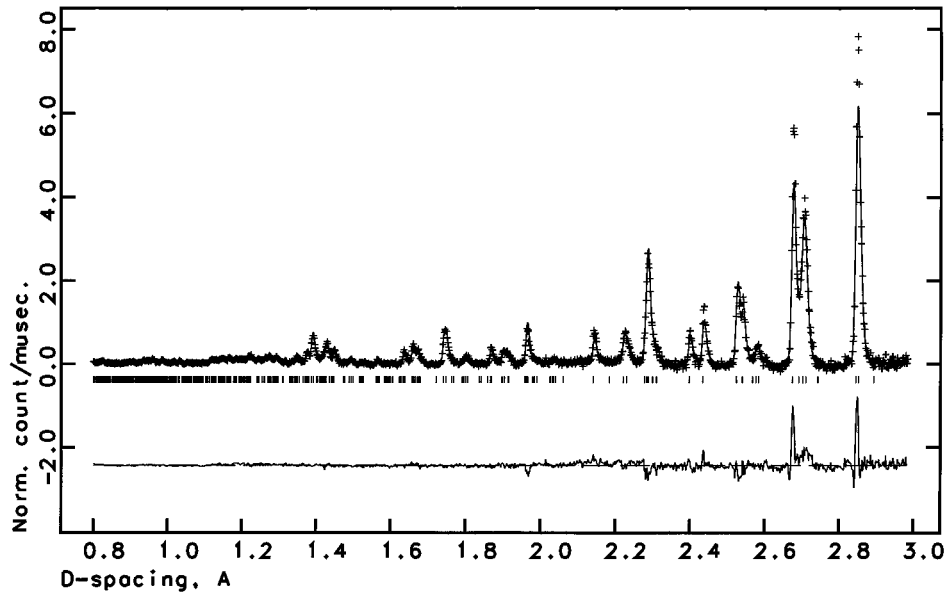

Figure 2. Neutron powder diffraction data (points) and the results of the Rietveld refinement (line). The lower line is the difference between experiment and theory.

(MP2) single-point calculations. Geometries for all six-membered-ring monomers were also optimized at the MP2 level, as were two cyclotriborazane dimers. Calculations on cyclotriborazane, cyclohexane, and cyclotrialumazane used Dunning's[28,29] polarized valence-double-ζ basis set (cc-pVDZ). Calculations on cyclotrigallazane monomer were carried out with the polarized valence-double-ζ basis set (pVDZ) of Schafer et al.[30] both for all atoms and for the case where Ga was treated by using the effective core potential basis set of Hay and Wadt[31] (ECP; this abbreviation will be taken to mean ECP only for the fourth row atom and pVDZ for all other atoms). Calculations for cyclotrigallazane dimers used only the ECP basis, as did calculations on 1,3,5-trigermacyclohexane. When we wish to generically refer to the two double-ζ basis sets employed, we will simply use "VDZ" to imply cc-pVDZ for cyclotriborazane and cyclotrialumazane and pVDZ for cyclotrigallazane.

Infrared frequencies were calculated at the RHF/VDZ level for all monomer geometries and are available as Supporting Information. Frequencies reported in the text have been scaled by a factor of 0.89 for NH and ND stretches and 0.93 for GaH and GaD stretches. All calculations were carried out with the Gaussian 94 program suite.[32]

Molecular Volume Calculations. The molecular volume was computed with use of the program GEPOL93.[33] van der Waals radii for H, C, N, Ga, and Ge were taken from the tabulation of Bondi.[34] The van der Waals radius of B was interpolated from the van der Waals radii of the first-row elements tabulated by Bondi.[34]

Results

Upon mixing $(GaH_3)NMe_3$ and NH_3, cyclotrigallazane was produced in high yield (eq 1).

$$GaH_3(NMe_3) + NH_3 \rightarrow {}^1/_3[H_2GaNH_2]_3 + NMe_3 + H_2 \quad (1)$$

Electron impact mass spectra (20 eV) of the perproteo- and perdeuteriocyclotrigallazane exhibited the parent peak at *m*/*e* 262 (24% abundance) and 273 (43%), respectively, which corresponds to the molecular weight of the trimer with the loss of one hydrogen/deuterium. Other fragment peaks were assigned to the loss of hydrogen, ammonia, or gallium from the trimeric, dimeric, or monomeric species. The infrared spectra of the protio and deuterio compounds displayed N−H(D) and Ga−H(D) stretching absorptions consistent with other gallazanes.[35] All vibrations of the protio and deuterio compounds agreed well with the theoretically predicted energies which are included as part of the Supporting Information. It is interesting to note that a different product, tentatively assigned as $H_2Ga(NH_3)_4GaH_4$, was reported from the reaction of Ga_2H_6 and NH_3.[36] This product has a different stoichiometry and distinct infrared stretching bands (3280, 3200, 1597, and 1237 cm^{-1}; 1941, 1809, and 780 cm^{-1}) compared to those of our product.

Cyclotrigallazane exhibits limited or no measurable solubility in hexane, benzene, toluene, and methylene chloride; however, related studies by Janik and Wells found good solubility in diethyl ether.[37] This contrasts the properties of the cycloborazanes, $[H_2BNH_2]_n$ ($n = 2-5$), which are soluble in a range of solvents depending upon the value of *n*.[38] The insolubility of this compound led to the earlier assumption of it being polymeric.[39] Although crystals of cyclotrigallazane are obtainable from the sublimation of the bulk product, the process is very slow. The lack of volatility could conceivably result from either the bulk product being composed of various oligomers or polymers with the trimer being the only sublimable oligomer or the existence of a substantial heat of sublimation for the trimer. Testing the solubility of the bulk material versus the sublimate over a range of solvents, however, failed to reveal

(28) Dunning, T. H. *J. Chem. Phys.* **1989**, *90*, 1007.
(29) Woon, D. E.; Dunning, T. H. *J. Chem. Phys.* **1993**, *98*, 1358.
(30) Schafer, A.; Horn, H.; Ahlrichs, R. *J. Chem. Phys.* **1992**, *97*, 2571.
(31) Hay, P. J.; Wadt, W. R. *J. Chem. Phys.* **1985**, *82*, 270.
(32) Frisch, M. J.; Trucks, G. W.; Schlegel, H. B.; Gill, P. M. W.; Johnson, B. G.; Robb, M. A.; Cheeseman, J. R.; Keith, T.; Petersson, G. A.; Montgomery, J. A.; Raghavachari, K.; Al-Laham, M. A.; Zakrzewski, V. G.; Ortiz, J. V.; Foresman, J. B.; Cioslowski, J.; Stefanov, B. B.; Nanayakkara, A.; Challacombe, M.; Peng, C. Y.; Ayala, P. Y.; Chen, W.; Wong, M. W.; Andres, J. L.; Replogle, E. S.; Gomperts, R.; Martin, R. L.; Fox, D. J.; Binkley, J. S.; Defrees, D. J.; Baker, J.; Stewart, J. P.; Head-Gordon, M.; Gonzalez, C.; Pople, J. A. *Gaussian 94 RevD.1*; Gaussian Inc.: Pittsburgh, PA, 1995.
(33) Pascual-Ahuir, J. L.; Tunon, I.; Silla, E. *J. Comput. Chem.* **1994**, *15*, 1127.
(34) Bondi, A. *J. Phys. Chem.* **1964**, *68*, 441.
(35) Storr, A.; Penland, A. D. *J. Chem. Soc., A* **1971**, 1237.
(36) Pulham, C. R.; Downs, A. J.; Goode, M. J.; Rankin, D. W. H.; Robertson, H. E. *J. Am. Chem. Soc.* **1991**, *113*, 5149.
(37) Janik, J. F.; Wells, R. L. *Inorg. Chem.* **1997**, *36*, 4135.
(38) Boddeker, K.; Shore, S.; Bunting, R. *J. Am. Chem. Soc.* **1966**, *88*, 4396.
(39) Storr, A. *J. Chem. Soc., A* **1968**, 2605.

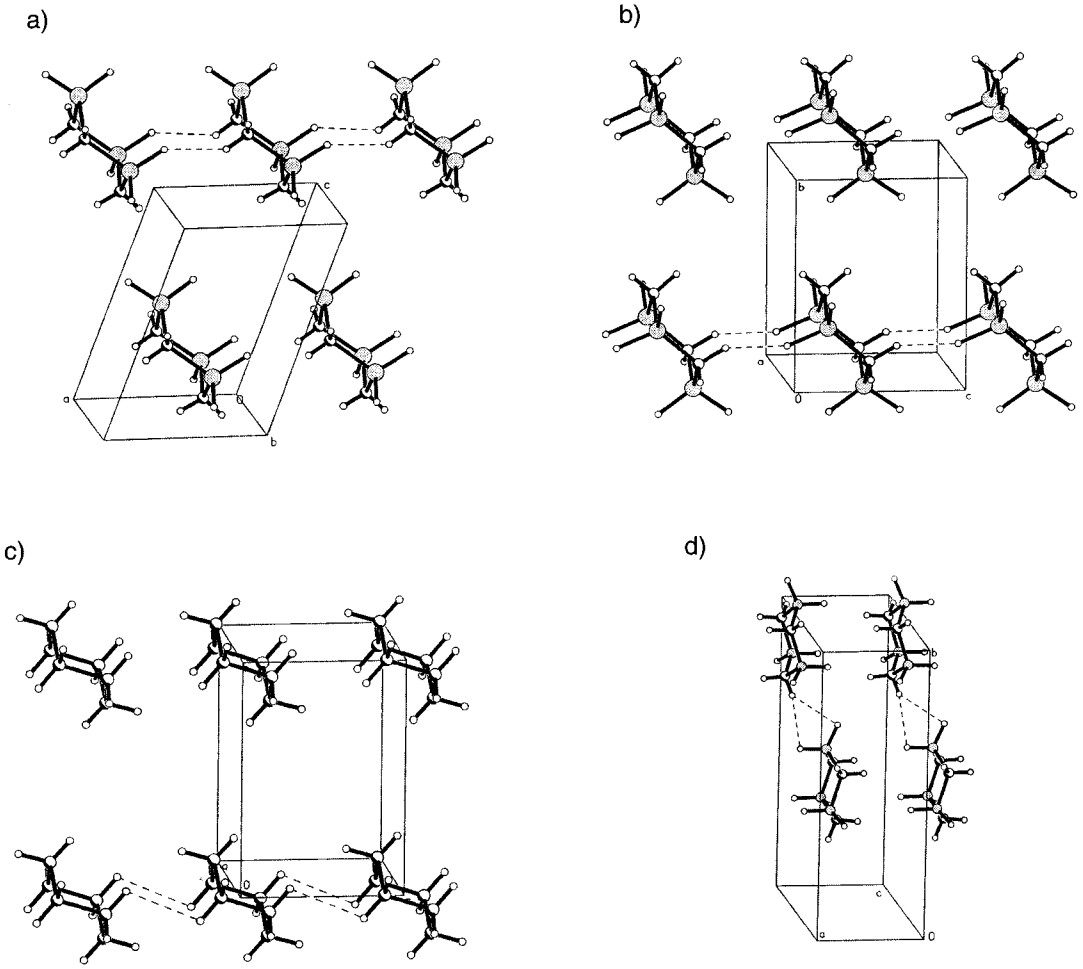

Figure 3. Packing arrangement in one plane of (a) cyclotrigallazane, (b) 1,3,5-trigermacyclohexane, (c) cyclohexane III, and (d) cyclotriborazane. In parts a, b, and d this plane contains the shortest H···H contacts which are indicated by the dashed lines. The dashed lines in part c do not represent the closest intermolecular H···H distances, but are indicated to emphasize the relationship to parts a and b.

Table 3. Intermolecular Distances and Angles in Cyclotrigallazane (from ND Data) for H···H Distances under 2.40 Å

atoms	distance (Å)
H2A−H3A	1.97(2)
H2A−H3E	2.37(2)
H2E−H3A	2.37(2)
atoms	**angle (deg)**
N2−H2A···H3A	146(2)
H2A···H3A−GA3	131(2)
N2−H2A···H3E	127(2)
H2A···H3E−GA3	126(2)
N2−H2E···H3A	131(2)
H2E···H3A−GA3	131(2)

any difference between the two. In addition to the solubility test, comparison of the *d* spacings of the bulk product from the powder diffraction pattern to those of the single crystals displayed no discrepancy. In the case of cycloborazanes, $[H_2BNH_2]_n$ ($n = 2-5$), these oligomers exhibit different *d* spacings from the powder diffraction patterns.[38] From these results, we conclude that the bulk product produced directly from eq 5 is primarily crystalline cyclotrigallazane.

Structure of $[H_2GaNH_2]_3$. The cyclotrigallazane molecule consists of alternating H_2Ga and NH_2 units forming a six-membered $(GaN)_3$ ring in a chair conformation. The $(GaN)_3$ ring lies on a crystallographic mirror plane. The average Ga−N distance (from XRD) is 1.981(7) Å, and the average N−Ga−N and Ga−N−Ga angles are 100.3(5)° and 117.1(3)°, respectively. These parameters compare well with other structurally characterized organogallazanes. For instance, the average Ga−N bond distances in $[H_2GaN(CH_2)_2]_3$,[40] $[H_2GaNMe_2]_2$,[41] and $[D_2GaN(CH_2)_3]_2$[42] are 1.97(19), 2.027(4), and 1.974(5) Å, respectively. The average N−Ga−N and Ga−N−Ga angles in $[H_2GaN(CH_2)_2]_3$[40] were 100° and 116°, respectively.

The X-ray and neutron diffraction data were collected at different temperatures, thus complicating direct comparison of the structural parameters. The greater spread in values for the neutron structure is not surprising considering the greater thermal motion at room temperature. The angles around gallium average 94.3°, which is 6° narrower than the corresponding values in the X-ray structure (100.3°). The agreement between the neutron structure and the X-ray structure is closer for N2 and N4; these angles differ by approximately 2°. The average of the six angles around each Ga and N atom in the X-ray structure is 108.7° whereas the analogous value is 107.2° for the neutron structure.

The Ga−D distances in $[D_2GaND_2]_3$ lie within 4σ of one another, but at 3σ differences appear between the axial and the equatorial bonds. The longest bond is Ga3−D3A, and at 1.59 Å it is 0.05 Å longer than the average for the equatorial set. This deuterium is involved in unconventional hydrogen bonding with a D−N group on a neighboring molecule—a factor which

(40) Harrison, W.; Storr, A.; Trotter, J. *J. Chem. Soc., A* **1966**, 1554.
(41) Greenwood, N.; Ross, E.; Storr, A. *J. Chem. Soc., A* **1966**, 706.
(42) Rendle, D.; Storr, A.; Trotter, J. *J. Chem. Soc., Dalton Trans.* **1973**, 2252.

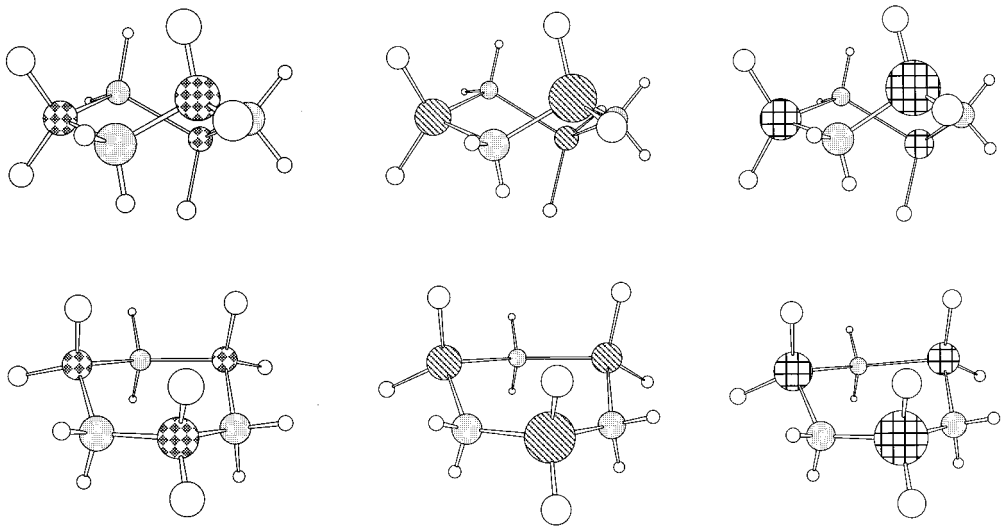

Figure 4. Twist-boat (above) and chair (below) structures for $\{[H_2BNH_2]_3\}_2$ (left), $\{[H_2AlNH_2]_3\}_2$ (center), and $\{[H_2GaNH_2]_3\}_2$ (right) as calculated at the RHF/VDZ level.

may contribute to its larger Ga−D length. The axial N2−D2A bond distance is 1.089 Å—somewhat longer than the 1.036 Å average for all of the N−H bonds. This hydrogen (deuterium) participates in hydrogen bonding with D3A, the axial D on Ga3.

The closest intermolecular D···D distance (between D3A and D2A), one on gallium and one on nitrogen, is 1.97(2) Å, which is significantly less than the sum of the van der Waals radii for two hydrogen atoms. Two other intermolecular D···D distances are also shorter than the van der Waals distance of 2.4 Å and are listed in Table 3. The packing diagram of cyclotrigallazane illustrating the close Ga−D···D−N distances along [100] is shown in Figure 3a. At 145° the intermolecular N2−D2A···D3A and is only slightly larger than the D2A···D3A−Ga3 angle (131°).

Theoretical Studies. The cyclotriborazane, cyclotrialumazane, and cyclotrigallazane monomers can exist in two stereoisomeric ring forms, namely chair and twist-boat. In carbocyclic conformational analysis, the chair is generally preferred over the twist-boat for steric reasons. In cyclohexane the chair is favored by 5.5 kcal/mol;[43] this preference derives from unfavorable H···H interactions across the ring between the unique "flagpole" positions, and also near-eclipsing interactions between substituents on the two pairs of nonflagpole positions.

In the azanes, on the other hand, these same interactions are modified by the opposite partial charges developed on the hydrogen atoms in question, i.e., the flagpole interaction involves a partially negatively charged hydrogen on the group 13 atom interacting with a partially positively charged atom on the group 15 atom, and this is a *favorable* electrostatic interaction. The electrostatic attraction is sufficient to overcome any steric bias in the azanes and, at the MP2/VDZ level, cyclotriborazane, cyclotrialumazane, and cyclotrigallazane prefer twist-boat forms over chairs by 0.9, 2.8, and 2.6 kcal/mol, respectively (the cyclotrigallazane number is 2.5 kcal/mol with the ECP basis).

As for the magnitude of the electrostatics, in the second row the difference in the relative conformer energies for cyclohexane compared to borazane is 7.5 kcal/mol. Because the ring geometries in these two compounds are not very different, it seems reasonable to ascribe this almost entirely to the favorable electrostatic interactions available in twist-boat cyclotriborazane but not twist-boat cyclohexane. To compare to cyclotrigallazane, we have also carried out calculations on isoelectronic 1,3,5-trigermacyclohexane. At the MP2/ECP level, 1,3,5-trigermacyclohexane prefers chair over twist-boat by 1.5 kcal/mol, indicating that the differential electrostatic effect is about 4 kcal/mol. The magnitude of this effect is reduced relative to the second row in part because the much longer bond lengths for the fourth-row compounds reduce nonbonded interactions, but probably also because there is some favorable electrostatic interaction even in 1,3,5-trigermacyclohexane. Mulliken population analysis[44] assigns charges of NH and GaH hydrogens in twist-boat cyclotrigallazane to be about 0.18 and −0.32 units, respectively; in twist-boat 1,3,5-trigermacyclohexane the charges of CH and GeH hydrogens are assigned as 0.10 and −0.24 units, respectively. This can be compared to cyclotriborazane (NH and BH hydrogen charges 0.14 and −0.14, respectively) vs cyclohexane (CH hydrogen charges 0.02 each), making it clear that the differential electrostatics are much larger in the second row.

Figure 4 provides structures of the azane twist-boats and chairs. Because it may be interesting to attempt to characterize the twist-boat global minima in the gas phase (e.g., by electron diffraction), their geometries are provided in the Supporting Information together with predicted infrared vibrational frequencies. However, as the focus of this article is on a crystal structure composed of chair monomers, we will not discuss the twist-boats in any further detail. MP2 geometries for the chair monomers differ only very slightly from RHF geometries (see Table 4 for the case of cyclotriborazane). Furthermore, cyclotrigallazane geometries were insensitive to using the pVDZ vs the ECP basis set. Both observations are consistent with our previous work on $[H_3BNH_3]_2$, $[H_3AlNH_3]_2$, and $[H_3GaNH_3]_2$.[15] Noting these points, and for computational efficiency, all dimer calculations were geometry optimized at the RHF level (with two exceptions discussed further below) and all cyclotrigallazane dimer calculations employed the ECP basis. To maintain consistency in making comparisons between monomers and the dimers discussed below, Table 3 provides selected geometrical data for the chair of cyclotrigallazane as calculated at the RHF/ECP level; the MP2 geometries are available in the Supporting Information along with predicted vibrational frequencies. Table 4 contains the corresponding values for $[H_2BNH_2]_3$, $[H_2AlNH_2]_3$, and $[H_2GeCH_2]_3$ as well as the experimental values for $[H_2BNH_2]_3$[45] and $[H_2GeCH_2]_3$.[46]

(43) March, J. *Advanced Organic Chemistry*, 4th ed.; John Wiley & Sons: New York, 1992; p 143.

(44) Mulliken, R. S. *J. Chem. Phys.* **1955**, *23*, 1833.

Table 4. Experimental and Calculated Bond Lengths (Å) and Angles (deg) for $[H_2BNH_2]_3$ and $[H_2GeCH_2]_3$ and Calculated Values for $[H_2AlNH_2]_3$

atoms M = B, Al, or Ge Y = C or N	exptl (XRD) for $[H_2BNH_2]_3$	calcd for $[H_2BNH_2]_3$[a,b]	calcd for $[H_2AlNH_2]_3$[a]	calcd for $[H_2GeCH_2]_3$[a]	exptl (XRD) for $[H_2GeCH_2]_3$[c]
M1−Y2	1.576	1.595 (1.596)	1.983	1.976	1.955(4)
Y2−M3	1.578	1.595 (1.596)	1.983	1.976	1.944(6)
M3−Y4	1.575	1.595 (1.596)	1.983	1.976	1.953(3)
M1−H1A	1.12	1.211 (1.216)	1.590	1.528	1.550
M3−H3A	1.12	1.211 (1.216)	1.590	1.528	1.594
M1−H1E	1.15	1.222 (1.225)	1.600	1.529	1.551
M3−H3E	1.16	1.222 (1.225)	1.600	1.529	1.546
Y2−H2A	0.89	1.008 (1.026)	1.012	1.097	1.131
Y4−H4A	0.88	1.008 (1.026)	1.012	1.097	1.084
Y2−H2E	0.91	1.008 (1.026)	1.014	1.096	0.966
Y4−H4E	0.90	1.008 (1.026)	1.014	1.096	0.979
Y4′−M1−Y4	107.3(1)	107.2 (106.8)	104.4	109.0	109.5(2)
Y2−M3−Y4	107.2(1)	107.2 (106.8)	104.4	109.0	110.0(3)
M1−Y2−M3	115.8(1)	118.0 (117.8)	125.0	115.0	112.7(3)
M3−Y4−M3′	116.0(1)	118.0 (117.8)	125.0	115.0	111.2(3)
H1A−M1−H1E	111.7(10)	113.8 (114.3)	121.3	108.4	109.4
H3A−M3−H3E	111.7(7)	113.8 (114.3)	121.3	108.4	103.1
H2A−Y2−H2E	105.1(10)	104.0 (103.6)	103.4	106.4	107.7
H4A−Y4−H4E	105.4(13)	104.0 (103.6)	103.4	106.4	100.7
H1A−M1−Y2	108.3(4)	108.8 (108.4)	108.3	109.4	109.6
H3A−M3−Y2	108.9(5)	108.8 (108.4)	108.3	109.4	116.5
H3A−M3−Y4	108.6(5)	108.8 (108.4)	108.3	109.4	105.0
H1E−M1−Y2	110.6(4)	109.0 (109.3)	106.7	110.3	109.4
H3E−M3−Y2	110.1(5)	109.0 (109.3)	106.7	110.3	115.4
H3E−M3−Y4	110.3(5)	109.0 (109.3)	106.7	110.3	105.7
H2A−Y2−M1	110.0(6)	110.4 (110.7)	108.6	108.3	106.7
H2A−Y2−M3	109.2(7)	110.4 (110.7)	108.6	108.3	109.6
H4A−Y4−M3	109.9(5)	110.4 (110.7)	108.6	108.3	112.3
H2E−Y2−M1	108.9(8)	106.5 (106.5)	104.5	109.2	111.0
H2E−Y2−M3	109.2(7)	106.5 (106.5)	104.5	109.2	109.5
H4E−Y4−M3	107.6(5)	106.5 (106.5)	104.5	109.2	109.9

[a] Calculations for $[H_2BNH_2]_3$ and $[H_2AlNH_2]_3$ at the RHF/cc-pVDZ level; calculations for $[H_2GeCH_2]_3$ at the MP2/ECP level. [b] MP2/cc-pVDZ optimized structural parameters in parentheses. [c] H1A and H1E were not found and the positions were calculated by assuming a tetrahedral geometry. Only a limited number of parameters were reported in the reference which explains the missing errors.

For the dimers, we considered four possible structures. There are almost certainly many more local minima on the dimer potential energy surface, but we restricted our focus to four structural types that seemed particularly relevant given the known crystal structures for cyclotriborazane, 1,3,5-trigermacyclohexane, and as presented here, cyclotrigallazane. We refer to these dimer structures as **A**, **B**, **C**, and **D**. Dimer **A** has C_{3v} symmetry and consists of two monomers stacked together so as to have three nearly collinear XH···HN hydrogen bonds formed from three axial XH hydrogens on one monomer and three axial NH hydrogen atoms on the other monomer. Dimer **B** also has C_{3v} symmetry but the monomer stacking is such that three axial XH hydrogens on one monomer form bifurcated hydrogen bonds with three axial NH hydrogens on the other monomer. Dimer **C** has C_s symmetry and is formed by allowing dimer **A** to relax so that one ring tilts relative to the other—this has the effect of swapping one axial−axial hydrogen bond for an equatorial−equatorial hydrogen bond between the two remaining axial−axial ones. Finally, dimer **D** has C_s symmetry and is formed by allowing dimer **B** to relax so that one ring "slips" relative to the other—this permits formation of two axial−axial hydrogen bonds at the expense of the three bifurcated hydrogen bonds present in **B** (if that change is favorable). Structures of these four dimers for all three azanes are provided in Figure 5 and selected geometrical data may be found in Supporting Information. In every case, dimerization is favorable, and the energies of dimerization are reported in Table 5.

One noticeable area of disagreement between theory and experiment concerns the length of heavy-atom-hydrogen bond lengths when the hydrogen atoms are engaged in H···H hydrogen bonding compared to not. Theory predicts essentially no effect from H-bonding on the X−H length, while experiment shows the expected lengthening. This discrepancy arises from a combination of three factors. First, as discussed below, the Hartree−Fock structures reproduce the hydrogen-bonding energetics well, but give dimer separations that are too large and hence probably fail to reproduce the X−H stretching potentials well. Associated with this point, the experiment measures the expectation value of the vibrational wave function for the X−H bond, while theory provides the equilibrium bond length—these may differ in systems with asymmetric potentials, such as those associated with hydrogen bonding. Finally, effects associated with the condensed phase not well reproduced in the dimer calculations (e.g., the Madelung field) may also play some role.

Discussion

Lewis base displacement and hydrogen elimination result from reactions of trimethylamine gallane with various primary or secondary amines. The initial product oligomerizes to produce cyclic gallazanes.[35,39,47]

$$n(GaH_3)NMe_3 + nRNH_2 \rightarrow (H_2GaNRH)_n + nNMe_3 + nH_2 \quad (R = Me, Et, Pr^n, Bu^n, Bu^i, Bu^s, Bu^t;\ n = 2, 3) \quad (2)$$

$$n(GaH_3)NMe_3 + HN\underbrace{(CH_2)_x}CH_2 \rightarrow [H_2GaN\underbrace{(CH_2)_x}CH_2]_n + nNMe_3 + nH_2 \quad (x = 1, 2, 3, 4;\ n = 2, 3) \quad (3)$$

(45) Corfield, P. W. R.; Shore, S. G. *J. Am. Chem. Soc.* **1973**, *95*, 1480.

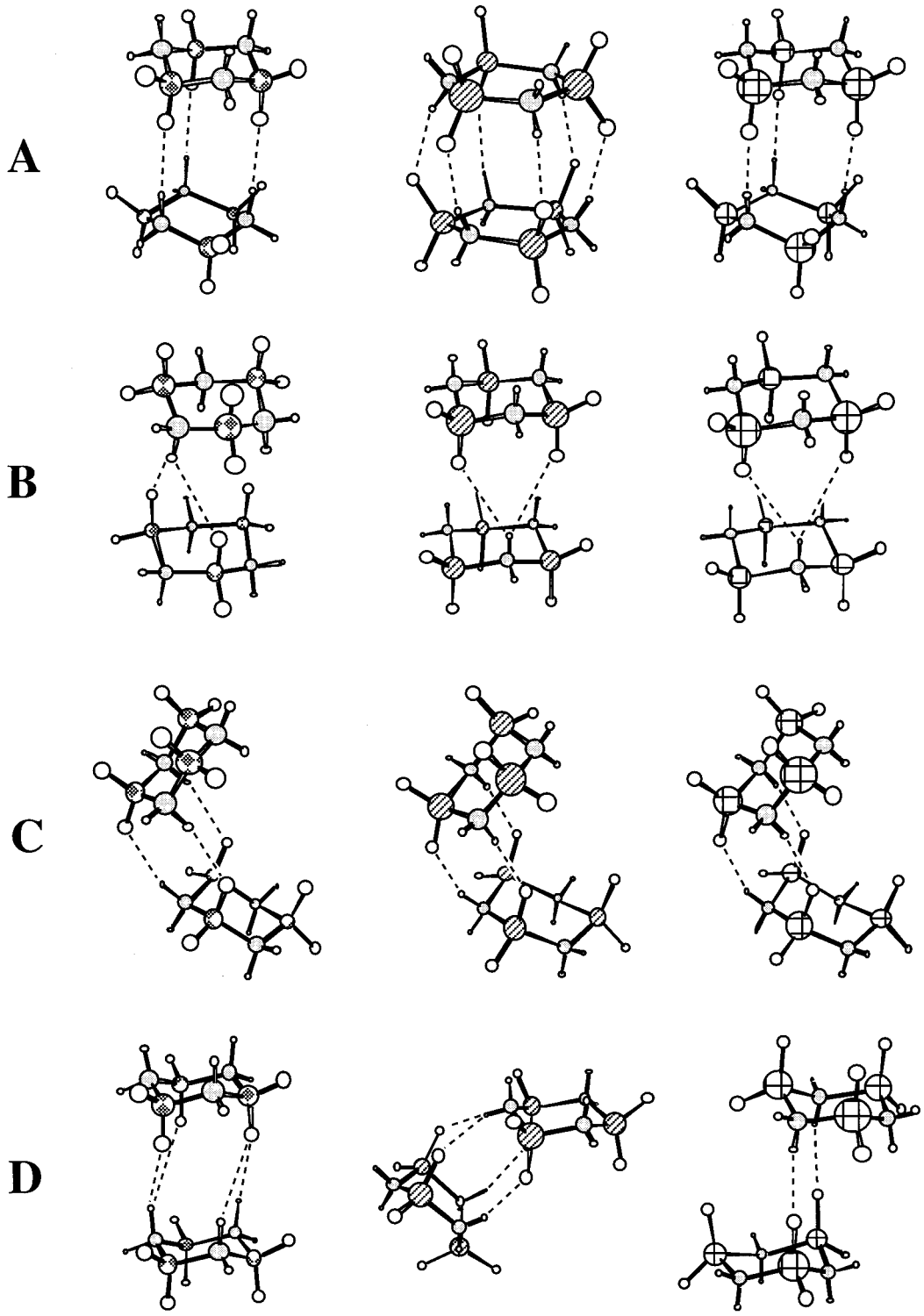

Figure 5. Structures of dimers **A**, **B**, **C**, and **D** of $\{[H_2BNH_2]_3\}_2$ (left), $\{[H_2AlNH_2]_3\}_2$ (center), and $\{[H_2GaNH_2]_3\}_2$ (right) as calculated at the RHF/cc-pVDZ level (borazane and alumazane) and the RHF/ECP level (gallazane). The intermolecular contacts are indicated by the dashed lines. For clarity in part B, only two of the six representative contacts are shown.

The reaction of ammonia with $(GaH_3)NMe_3$ occurs in an analogous fashion; however, the characterization of cyclotrigallazane is complicated by its limited solubility and volatility. The original report of this reaction suggested that the product was polymeric.[48] X-ray and neutron powder diffraction of the product establishes that the cyclic trimer is the only crystalline phase present. The similar solubilty, spectroscopy, and volatility of single crystals of $[H_2GaNH_2]_3$ to those observed for the powdered product provide further support that the powder is composed primarily of cyclotrigallazane.

Comparison of Crystal Structures of Cyclotriborazane, Cyclohexane III, 1,3,5-Trigermacyclohexane, and Cyclotrigallazane. In cyclotrigallazane, the closest intermolecular bonds

(46) Schmidbaur, H.; Rott, J.; Reber, G.; Müller, G. *Z. Naturforsch.* **1988**, *436*, 727.

(47) Storr, A.; Thomas, B.; Penland, A. *J. Chem. Soc., Dalton Trans.* **1972**, 326.

(48) Biswas, D. R.; Ghosh, C.; Layman, R. L. *J. Electrochem. Soc.* **1983**, *130*, 234.

Table 5. Dimerization Energies (kcal/mol) at the MP2//RHF Level of Theory[a,b]

dimer	$\{[H_2BNH_2]_3\}_2$, M = B	$\{[H_2AlNH_2]_3\}_2$, M = Al	$\{[H_2GaNH_2]_3\}_2$, M = Ga
A	−7.2 (−8.1)[c]	−9.9	−7.4
B	−4.8 (−6.1)[c]	−4.1	−3.8
C	−8.2	−9.5	−7.8
D	−4.8	−12.5	−4.1

[a] Calculations for $\{[H_2BNH_2]_3\}_2$ and $\{[H_2AlNH_2]_3\}_2$ used the cc-pVDZ basis set; calculations for $\{[H_2GaNH_2]_3\}_2$ used the ECP basis set. [b] Relative to chair monomers. See Figure 5 for structures. [c] Dimerization energy using MP2/cc-pVDZ optimized geometries.

between adjacent molecules create an α-network[3] parallel to the crystallographic *a*-axis in which each molecule participates in four unconventional hydrogen bonds. It is not difficult to envision that this packing pattern obtains to maximize this strong, cooperative intermolecular interaction. Inspection of the structure in the other two crystallographic directions reveals that each H−Ga group may be paired with a unique H−N group. As shown in Figure 3a, one unit cell translation along the *c* axis causes the H_2Ga end of one molecule to contact the H_2N ends of two six-membered rings. The orientation of the six-membered rings relative to this translation is such that the H_2-Ga fragment almost perfectly bisects the NH_2 groups on two adjacent molecules. As shown in Figure 3a one of the Ga−H···H−N distances is quite long (3.67 Å), but the other is close (2.68 Å).

The trimers bisected by the mirror plane at 0.25 along the *y* axis have a common direction of the dipole moment. The 2_1 screw axis allows the next layer along *b* (at 0.75) to pack efficiently and rotates the dipole moment of the plane by 180°. Along this direction no interactions are shorter than the van der Waals distance.

The similar molecular shape for cyclotrigallazane, 1,3,5-trigermacyclohexane,[46] cyclohexane,[49−51] and cyclotriborazane[45] leads to similar packing arrangements. This is expecially true for cyclotrigallazane, 1,3,5-trigermacyclohexane, and cyclohexane III (cyclohexane exists in five known polymorphs, two (I and II) are found at ambient pressures and three at pressures between 5 and 18 kbar[49−51]). Figure 3 illustrates views of the packing of the molecules in a plane that contains the closest intermolecular distances for all but cyclohexane. For cyclotrigallazane and 1,3,5-trigermacyclohexane, not only is the overall packing arrangement similar, but the closest intermolecular distances occur between analogous, oppositely charged hydrogens on adjacent molecules. These similarities allow us to assign the quantitative difference in H(D)···H(D) distances (1.97(2) Å in cyclotrigallazane and 2.20 Å in trigermacylcohexane) to the formation of an unconventional hydrogen bond in cyclotrigallazane.

Although cyclotriborazane also forms an α-network of close intermolecular distances, the direction of this network lies parallel to the plane of the molecules, Figure 3d, and, more significantly, the pattern of individual H···H bonds differs. Rather than exhibiting a unique interaction between one hydride and one proton, borazane exhibits a bifurcated H···H bond in which the H(N) almost perfectly bisects a BH_2 on the adjacent molecule and forms two, equivalent interactions. All atoms involved in this intermolecular interaction are coplanar. It is noteworthy that theoretical studies of $[H_3BNH_3]$ established that favorable dimerization occurs through bifurcated unconventional hydrogen bonds.[15]

Calculation of the Kitaigorodsky packing coefficient,[52] C_k, for these structures yields 0.63, 0.68, 0.68, and 0.73 for cyclotriborazane, cyclohexane II (chosen for this comparison because it was characterized at atmospheric pressure and, unlike cyclohexane I, is fully ordered), trigermacyclohexane, and cyclotrigallazane, respectively. Although we see that cyclotrigallazane is the most efficiently packed structure by this measure, the packing efficiency does not correlate with the calculated strength of the H···H bonding (vide infra). At least in part, this is because the close intermolecular distances are found only along one crystallographic direction.

What does display at least a *qualitative* correlation with the calculated strength of the H···H bonding is the melting point (T_m). In general, the correlation of melting point with cohesive energy must be done with caution. A high T_m can result from a large melting enthalpy or from a low entropy of melting; the latter situation is common with disordered crystals.[53] A relevant example is cyclohexane I, which is stable from its melting point at +6.55 to −87 °C, is dynamically disordered, and exhibits a low melting entropy of 2.3 eu.[49] The result is a T_m that is higher than the melting point observed for fully ordered trigermacylcohexane (T_m = −14 °C), despite the replacement of three carbons with the heavier, more polarizable germanium. On the basis of the calculations described in this paper, neither exhibit any tendency to form intermolecular bonds stronger than van der Waals interactions. Both cyclotriborazane and cyclotrigallazane have melting points ≥140 °C. Above 140 °C, both solids undergo chemical reactions, which for cyclotrigallazane ultimately leads to nanocrystalline GaN. Theory does suggest that both cyclotriborazane and cyclotrigallazane form unconventional hydrogen bonds, and we speculate that this leads to a higher cohesive energy and as a result a higher T_m.

Assessing the Importance of Unconventional Hydrogen Bond Formation in Cyclotrigallazane. Prior to focusing on specific geometric details, it is worth noting that the RHF dimers are expected to have inaccurately large intermonomer separations (in part because this level of theory fails to take account of attractive dispersion forces). In our earlier work on $[H_3BNH_3]_2$, $[H_3AlNH_3]_2$, and $[H_3GaNH_3]_2$,[15] we found that intermolecular H···H hydrogen bond distances typically shortened by 0.2 Å on going from the RHF to the MP2 level of theory. However, the energetic effect of that shortening was usually less than 1 kcal/mol at the MP2 level of theory.[15]

To evaluate this effect for the present systems more completely, we carried out MP2/cc-pVDZ optimizations on cyclotriborazane dimers **A** and **B**. Selected geometrical details for these structures are contained in the Supporting Information, and the fully optimized dimerization energies for these and all other structures are listed in Table 5. As we found for $[H_3BNH_3]_2$,[15] the individual cyclotriborazane geometries change very little at this level. The intermolecular H···H hydrogen bond distances, on the other hand, change enormously, by 0.37 and 0.54 Å for dimers **A** and **B**, respectively! The resulting H···H distance in **B** is 2.430 Å, which is in fair agreement with the experimental value of 2.29(2) Å derived from a cyclotriborazane crystal structure showing a bifurcated stacking arrangement like that calculated for **B**.

Despite the significant geometrical changes, the energetic consequences of reoptimization are not especially large. The

(49) Kahn, R.; Fourme, R.; André, D.; Renaud, M. *Acta Crystallogr.* **1973**, *B29*, 131.
(50) Wilding, N. B.; Hatton, P. D.; Pawley, G. S. *Acta Crystallogr.* **1991**, *B47*, 797.
(51) Wilding, N. B.; Crain, J.; Hatton, P. D.; Bushnell-Wye, G. *Acta Crystallogr.* **1993**, *B49*, 320.
(52) Kitaigorodsky, A. *Molecular Crystals and Molecules*; Academic Press: New York, 1973; p 553.
(53) Gavezzotti, A. *Acc. Chem. Res.* **1994**, *27*, 309.

MP2 cyclotriborazane dimerization energies increase in magnitude by only 0.9 and 1.2 kcal/mol for **A** and **B**, respectively, on going from the RHF to the MP2 geometries. Because of the significant computational expense associated with MP2 optimizations (even for these fairly high-symmetry dimers), we did not reoptimize any other dimer geometries, and we restrict further discussion to RHF structures. We anticipate predicted RHF intermolecular separations for other dimers to be in error probably by a similar margin to that found for cyclotriborazane dimers **A** and **B**, and we further expect that reported dimerization energies will be underestimated by about 0.3 to 0.4 kcal/mol per hydrogen bond.

The geometries of the cyclotriborazane and cyclotrigallazane dimers **A** are quite similar, as are the predicted binding energies. Cyclotrialumazane, on the other hand, is predicted to flatten both six-membered rings in order to enjoy six H···H contacts (Figure 5). This appears to illustrate that AlH···HN interactions are somewhat stronger than in the analogous boron or gallium cases, consistent with our earlier observations for the $[H_3XNH_3]_2$ systems.[15] The extra H···H contacts in cyclotrialumazane dimer **A** make it more stable than dimer **C** by 0.4 kcal/mol. For cyclotriborazane and cyclotrigallazane, on the other hand, dimers **C** are predicted to be more stable than **A** by 1.0 and 0.4 kcal/mol, respectively. Although it is speculative to interpret such small energy differences, the apparently stronger H···H hydrogen bonds in dimers **C** compared to **A** may be associated with the less linear XH···HN arrangement in **C**. As noted by Richardson et al.,[14] the maximum position of electron density in the XH bond occurs *between* the two atoms, so that XHH angles more acute than NHH angles are favored; this is exactly the situation observed in dimers **C**, with angle differences of about 30° for the 2-fold symmetric H···H hydrogen bonds, and a more variable value for the unique H···H hydrogen bond.

When dimer **B** of cyclotrialumazane is allowed to relax from C_{3v} to C_s symmetry, one monomer ring flips from chair to boat (because of the C_s symmetry constraint, it cannot further relax to twist-boat) and the resulting dimer "**D**" is considerably more stable than **B** (and clearly only a small portion of that is related to the ring flip). This behavior is qualitatively quite different than that calculated for boron and gallium; such qualitative differences between these group 13 elements have been pointed out before.[54]

When dimer **B** is allowed to relax in the cyclotriborazane system, there is a very slight shift of one ring relative to the other that shortens one of the bifurcated H···H hydrogen bonds in **D**. The energy drops by less than 0.1 kcal/mol for this change, however. In the cyclotrigallazane system, on the other hand, the shift in ring positions is significant in **D**, and leads to two approximately collinear NH···HX hydrogen bonds nearly 0.8 Å shorter than the bifurcated ones found in **B**.

It is tempting to speculate that this different behavior for the latter two azanes rationalizes their different crystal packing arrangements—as noted above, cyclotriborazane stacks monomers in geometries similar to **B**, while cyclotrigallazane has a stacking arrangement much more similar to that of **D**. However, the energy difference between dimers **B** and **D** is only 0.3 kcal/mol for cyclotrigallazane, and it is clear that other crystal packing effects could easily dominate this effect and provide more of a driving force for the observed crystal morphology.

To explore this latter point in somewhat more detail, it must be kept in mind that the gas-phase dimerization energies for these systems can provide at best a rather crude estimate of the crystal packing energy, since no account is taken of cooperative effects involving more than two monomers. For instance, cooperative effects have been calculated to improve hydrogen bonding in stacks of amides[55] and it is further known that structures of weakly interacting dimers can change substantially on going from the gas phase to the condensed phase.[56] Even with all of these caveats in mind, however, dimer calculations can offer qualitative information on geometrical details and semiquantitative information on intermolecular interactions, and it is in this spirit that these azane calculations should be interpreted. On the basis of the dimerization energies in Table 5, and given the expected underestimation of the binding energy at the RHF level, we calculate that the H···H interaction energy in cyclotriborazane and cyclotrigallazane is about 3 kcal/mol per hydrogen bond.

Relationship between Cyclotrigallazane and Cubic GaN. The combined effect of the molecular structure and the crystal packing create an interesting correlation to the solid state compound, gallium nitride. In cyclotrigallazane, each Ga is bonded intramolecularly to two nitrogens. Although the unconventional hydrogen bonds lack strong directionality, the intermolecular connections, outlined above, correlate with the third and fourth coordination sites of gallium in gallium nitride. In essence, one can consider $[H_2GaNH_2]_3$ to be a "hydrogenated" cubic GaN structure. In all three crystallographic directions, the topology of the cyclotrigallazane structure correlates with the unknown zinc blende polymorph rather than with the known wurtzite phase. The ramifications of this relationship during the dehydrogenation process include the formation of nanocrystalline GaN enriched in the cubic close-packed phase.[18]

Conclusions

In the solid state cyclotrigallazane exists in the chair conformation and individual molecules are connected by unconventional hydrogen bonds (between a Ga−H and an N−H group) in an α network parallel to the crystallographic *a* axis. Powder neutron diffraction analysis of the perdeuterio analogue established an intermolecular D···D distance of 1.97(2) Å. In the gas phase, MP2/cc-pVDZ calculations predict twist-boats to be preferred over chairs for cyclotriborazane, cyclotrialumazane, and cyclotrigallazane by 0.9 to 2.6 kcal/mol. Apparently crystal packing considerations outweigh this preference given the experimentally determined crystal structures of cyclotriborazane and cyclotrigallazane (of course, crystal structures incorporating twist-boats may yet be discovered). For the four dimer motifs considered, dimer geometries and binding energies are quite sensitive to the group 13 element. For cyclotriborazane and cyclotrigallazane, calculations suggest that each H···H hydrogen bond contributes about 3 kcal/mol to the binding energy (relative to chair monomer); this value is very slightly higher for cyclotrialumazane. The strengths of these interactions are comparable to conventional hydrogen bonds, suggesting that they can be added to the crystal engineer's arsenal for effecting the structure of molecular crystals.

Acknowledgment. This work was supported by the National Science Foundation (CHE-961501). The authors wish to acknowledge Prof. Doyle Britton for helpful discussions. We are grateful for high-performance vector and parallel computing resources made available by the Minnesota Supercomputer Institute and the University of Minnesota-IBM Shared Research

(54) Raston, C. L. *J. Organomet. Chem.* **1994**, *475*, 15.

(55) Guo, H.; Karplus, M. *J. Phys. Chem.* **1994**, *98*, 7104.

(56) Leopold, K. R.; Canagaratna, M.; Phillips, J. A. *Acc. Chem. Res.* **1997**, *30*, 57.

Project, respectively. C.J.C. thanks the Alfred P. Sloan foundation for funding. Support by BES/DOE for the neutron diffraction work at the Manuel Lujan, Jr. Neutron Scattering Center, Los Alamos National Laboratory under contract number W-7405-ENG-36 is also acknowledged.

Supporting Information Available: Listings of X-ray crystallographic data, neutron crystallographic data, atomic coordinates, thermal parameters, calculated Cartesian coordinates for all monomers and dimers, and infrared frequencies for all monomers; calculated distances and angles for dimers and monomers where monomer data include both chairs and twist-boats (31 pages). See any current masthead page for ordering and Internet access instructions.

JA971478E